Microwave assisted sintering of Na-β''-Al_2O_3 in single mode cavities: insights in the use of 2450 MHz frequency and preliminary experiments at 5800 MHz

Cecilia Mortalò[1], Roberto Rosa[2*], Paolo Veronesi[3], Stefano Fasolin[1], Valentina Zin[1], Silvia Maria Deambrosis[1], Enrico Miorin[1], Georgios Dimitrakis[4], Monica Fabrizio[1], Cristina Leonelli[3]

[1]National Research Council, Institute of Condensed Matter Chemistry and Technologies for Energy, Corso Stati Uniti 4, 35127, Padova, Italy

[2]Department of Sciences and Methods for Engineering, University of Modena and Reggio Emilia, Via G. Amendola 2, 42100 Reggio Emilia, Italy

[3]Department of Engineering "Enzo Ferrari", University of Modena and Reggio Emilia, via P. Vivarelli 10, 41125, Modena, Italy

[4]Department of Chemical and Environmental Engineering, The University of Nottingham, University Park, Nottingham NG7 2RD, United Kingdom

*corresponding author: Tel.: +390522523558; E-mail: roberto.rosa@unimore.it

Abstract

Microwave assisted sintering of Na-β''-Al_2O_3 in single mode cavities was accurately investigated. The use of single mode cavity allowed monitoring the parameters affecting the sintering process, like the forward power, together with the temperature evolution, making possible to perform energy efficiency and specific energy consumption evaluations.

Experiments have been performed at the frequency of 2450 MHz, but preliminary results are also reported using the higher frequency of 5800 MHz, in order to investigate its effect on important parameters like the power density distribution as well as the penetration depth, which are responsible of the resulting heating rate and sintering outcome.

Dielectric properties of the powders were measured as a function of temperature in order to partially predict and support the understanding of their experimental heating behaviour. Furthermore, dielectric properties provide the fundamental information needed for the multiphysics numerical simulation, performed with the aim to reach insights into the power density evolution in the specimen as sintering proceeds.

Keywords: A. Microwave processing; A. Sintering; C. Dielectric properties; D. β-Al_2O_3.

1. Introduction

Sodium β–alumina attracted remarkable attention from the scientific community during the last decades for a wide variety of applications, including batteries, gas sensors and high ε-dielectrics based devices [1]. Its crystal structure consists of alternating layers of alumina spinel blocks and parallel conduction planes where Na^+ ions are free to move. The movement of the sodium ions through the conduction planes results in a high ionic conductivity in this material, making it extremely appealing as solid electrolyte in electric energy storage (EES) systems [2,3]. Indeed, the Na-based batteries are considered the most promising alternatives to lithium-ion technology, as a consequence of the highly abundant sodium resources, low cost and comparative performances with respect to Li-based ones [4,5]. These systems are based on the use of β/β''-Al_2O_3 as solid electrolyte membrane that selectively allows sodium ions transport between a positive and a negative electrode [6]. Even if it is well established that β''-Al_2O_3, having rhombohedral crystal structure (*R*3*m*; a_0 = 0.560 nm, c_0 = 3.395 nm), exhibits a higher sodium ionic conductivity with respect to the hexagonal ($P6_3/mmc$; a_0 = 0.559 nm, c_0 = 2.261 nm) β-Al_2O_3 phase [4,6], most of both sodium-sulfur (Na-S) [7,8] and ZEBRA (i.e. ZEolite Battery Research Africa) [9,10] batteries, even the most recently developed [11], reversibly charge and discharge electricity via sodium ions transport across a solid electrolyte that is typically composed of a mixture of β-Al_2O_3 and β''-Al_2O_3 phases, usually doped with low valence elements.

Apart from the electrical performances as solid electrolyte, sodium β-alumina has been recently considered for high ε-dielectrics based devices as a consequence of its high capacitance with strong polarization perpendicular to the conduction planes [12]. Indeed, Pal and co-workers have applied sodium β-alumina as the passive dielectric layer in a thin film transistor (TFT) [13]. The high dielectric constant (ε) of sodium β-alumina improved greatly the performance of the TFT especially at low voltage operation conditions.

Lastly, sodium β-alumina has been recently applied as an electrolyte in solid-state electrochemical gas sensor for the quantitative determination of carbon dioxide [14], opening up new potential applications.

Despite the huge range of applications, several challenges based on the processing steps, i.e. powders synthesis and the subsequent high temperature sintering process [10], still hamper the effective market penetration of the sodium beta alumina related technologies. Although solid-state reaction (SSR) method [15], still remains the method of choice for large scale production of Na-β''-Al_2O_3, it is significantly high energy and time demanding. Thus, several techniques have been developed and optimized namely, sol-gel process [16], mechanochemistry [17], spray pyrolysis and combustion synthesis [18,19]. Although most of these techniques allows obtaining more homogeneous powders with a higher surface area, the desired β'' phase usually coexists with the β one into the reaction products. However, regardless the synthetic procedure, to achieve optimal physical, mechanical and electrochemical properties, powders need to be well sintered. The common sintering processes require time prolonged and high temperature conditions (> 1600°C) that usually cause unwanted sodium evaporation, leading to compositional variations and loss of ionic conductivity, excessive grain growth and extremely high energy consumptions [4]. Recently, some authors demonstrated that the introduction of MgO [20], NiO [21], or ZrO_2-based oxides [11, 22-24] as sintering aids could limit excessive grain growth and improve the mechanical properties of the densified samples. However, in many cases the electrical performance of final sintered specimen was deteriorated, due to the presence of some secondary phases [21, 22]. Hence, further improvements are still required in

order to develop suitable methods for fabricating β-alumina based materials with well-controlled stoichiometry and microstructure. The present work aims to address exactly these latter sintering-related issues. Particularly, among the less conventional sintering techniques, which have been proposed, the use of microwave (MW) energy is probably the one characterized by the highest degree of maturity. Indeed, during the last three decades MW heating started gaining increasing research interest, not only in the synthesis of inorganic compounds [25,26], but also for the sintering of a wide variety of materials including ceramics [27-30], metals [31-36] as well as several kinds of composites [37-39], since numerous advantages have been claimed and reported with respect to conventional heating procedures [40,41]. These include, for example, enhanced diffusivity and decreased sintering temperatures, which therefore significantly reduce processing times as well as the required energy consumption.

However, although the widespread application of microwave energy to ceramic materials, scientific reports devoted to detailed and exhaustive investigation on the microwave assisted sintering process for solid Na-β''-Al_2O_3-based electrolyte, are still surprisingly scarce [42], most of which being devoted to the contemporary synthesis and sintering [43,44]. Moreover, even more surprising is the lack of any temperature measurement details, together with the complete absence of emitted power profiles during sintering experiments, making any energy efficiency evaluation and comparison with traditional techniques, not possible at all.

This is, in all likelihood, a direct consequence of the fact that the instrument of choice in all of the aforementioned research activities was a domestic microwave multi-mode applicator. However, in order to investigate in full details and consequently optimize all the parameters involved in the sintering process, like the forward microwave power, together with the exact temperature measurement, the use of a scientific single mode microwave cavity is mandatory.

Thus, this work is focused on the use of single mode microwave applicators for the sintering of Na-β''-Al_2O_3-based powders, prepared by an optimized SSR method [45].

Particularly, the most conventionally employed 2450 MHz frequency was investigated in detail, but preliminary experiments at the newly proposed 5800 MHz frequency are presented as well. The latter must be considered preliminary results because of the lower degree of controllability of the heating rate that we experienced in our setup.

The experimental activity was accompanied by the measurement of the dielectric properties of the starting powders as a function of temperature (up to 1200 °C at 2.45 GHz) and supported by numerical simulation. These latter activities were performed with the aim to better understand the effect of the two different frequencies on the power density distribution, as well as on the power penetration depth and subsequently on the sintering behaviour of Na-β''-Al_2O_3-based powders.

2. Experimental

2.1 Powders synthesis

Pure Na-β''-Al_2O_3 powders stabilized by Li^+ cations, with the chemical formula of $Na_{1.67}Li_{0.33}Al_{10.67}O_{17}$, were prepared by SSR method according to the procedure recently optimized by some of the present authors [45].

Briefly, γ-Al_2O_3 (Alfa Aesar, 99.97%), Na_2CO_3 (Alfa Aesar, ACS, ≥99.5%) and Li_2CO_3 (Sigma Aldrich, ACS reagent, ≥99.0%) in the opportune stoichiometric amounts were dispersed in absolute anhydrous ethyl alcohol (Carlo Erba, Italy). The mixture was then ball-milled for 24 hours in a planetary ball-milling apparatus (Pulverisette 7, Fritsch) at 350 rpm into a ZrO_2 jar containing ZrO_2 balls (10 mm diameter). After 24 h grinding, the powders were calcined at 1250 °C (Nabertherm HT 04/17 furnace) with a heating rate of 5°C/min and an isothermal heating period of 12 h. These powders were briefly indicated as NaBA.

An additional ball milling treatment (24 h at 350 rpm) was performed on the as calcined powders dispersed in ethanol, in order to reduce the particles size. The selected acronym for these double milled powders was NaBADM.

2.2 Dielectric properties, MW-assisted sintering and numerical simulation

In order to justify the exploitation of microwave energy as heating source in the sintering experiments, as well as to obtain supporting information for the subsequent laboratory experiments and for the simplified numerical simulations, the dielectric properties of the as-synthesised powders were first of all measured at 2470 MHz frequency (i.e. very close to the allocated ISM band frequency of 2450 MHz, and however comprised in the operational frequency range of the employed magnetron), in the temperature range 20-1200°C by the cavity perturbation technique [46]. The experimental set up employed is detailed elsewhere [47]. In brief, it consists of a cylindrical copper resonant cavity of dimensions that are specific for the production of the 2470 MHz resonant frequency. Additional components include a tube furnace (able to operate up to 1300°C), a vector network analyzer (VNA, HP 8753C), a computer with a customize program to control the system and a vertical sample actuator used to move the sample holder to the cavity and to the furnace. A representative and fixed amount of powders (*ca.* 0.2 g) was packed in a quartz tube, which was then heated at the desired temperature and subsequently inserted into the resonant cavity by means of the automatic actuator. Three measurements were replicated for each temperature value.

The open-ended coaxial probe technique [46] was instead employed to measure dielectric properties at 5800 MHz frequency, from room temperature up to *ca.* 200 °C (in order to avoid any possible deterioration of the probe due to higher temperatures) by means of an Agilent 8753D network analyser connected to an Agilent 85070E dielectric kit probe. During these measurements, the temperature was monitored by an optical fibre (Neoptix Reflex four channels, temperature range -50 ÷ +250°C, Qualitrol company, Canada) directly inserted into the powders. The measurements were performed on loose powders, which were opportunely compacted once in contact with the steel dielectric probe. The measurements were performed in triplicate during cooling at every 25 °C step.

Both 2450 and 5800 MHz sintering experiments were conducted in rectangular TE_{10n} single-mode applicators (*i.e.*, with a transverse electrical mode presenting only one semisinusoidal variation of the electric field in the *x* direction, 0 variations in the y direction and n variations in the z direction, with

n = 2 or 3 in the experimental setup used). Briefly, they consist of a magnetron generator (MKS-Alter, Reggio Emilia, Italy), with an output power level ranging from 100 to 1000 W (for the 5800 MHz one) and from 500 to 3000 W (for the 2450 MHz one), connected to a three-port circulator and to a three-stubs tuner (MKS-Alter, Reggio Emilia, Italy). The cavity for heat treatments consisted of a rectangular resonant applicator, based on the standard WR-340 waveguide (i.e. 86 x 43 mm^2 section, in the case of a 2450-MHz frequency) or the WR-159 waveguide (i.e. 40 x 20 mm^2 section, in the case of a 5800-MHz frequency). In both applicators, the three-stubs tuner and an additional shorting plunger allow manual impedance matching operations in order to modify the electromagnetic field distribution along the cavity. **Figure 1a** shows the two microwave single mode applicators used for this study.

The microwave-assisted sintering experiments were carried out on green discs of approximately 14 mm diameter and 3 mm height obtained by uniaxial pressing of *ca*. 1g of Na-β''-Al_2O_3 powders into a stainless-steel mould at 410 MPa.

The arrangement of the specimen inside the single mode cavity was adjusted in order to realize a hybrid heating [48], as depicted in **Figure 1b** (in the representative example of 5800 MHz frequency case). Particularly, the green sample was placed in the centre of a rectangular alumina-based refractory container and surrounded from the four sides and the bottom by chemically vapour deposited (CVD) silicon carbide (SiC, Rohm and Haas, USA) microwave co-absorber pieces. It was separated from the direct contact with the SiC basement by means of loose powders of the same composition of the specimen itself. On the top of it, a further layer of the same refractory material, with a hole for temperature measurement, was used to increase the thermal insulation. Surface temperature of the β-allumina pellet was monitored by a sapphire fibre (Mikron M680 Infraducer, temperature range 600-1900 °C, Mikron Infrared, Oakland, NJ, USA). The latter was positioned in contact with the sample, through the cylindrical waveguide section under cut-off conditions, positioned on the top of each single mode cavity (in **Figure 1c**, the case of a 5800 MHz frequency experiment is reported as a representative example). The geometric characteristics and the amounts

of SiC susceptors as well as of refractory material employed in the experiments performed at both frequencies are reported in **Table 1**. The same data were then used to perfectly reproduce the set-up of the experimental approach in the designed model geometry.

Table 1. Geometric characteristics and amount of SiC susceptor and alumina-based refractory container employed for the arrangement of the specimen in each single mode applicator.

	n° of 10x6.5x2 mm^3 SiC pieces	Total weight of SiC employed (g)	Dimension of Al_2O_3-based refractory container (mm^3)
2450 MHz	14	5.6	49.5 x 58 x 40
5800 MHz	14	5.6	38 x 40 x 18

The model geometries perfectly reproducing the set-up used for the experiments performed at both 2450 and 5800 MHz frequencies are sketched in **Figure 2**. In both cases, microwaves input port is placed on the left, as indicated by the black arrows in **Figure 2**. The 3D final models were meshed using triangular advancing front elements (regular refined mesh), with the compacted Na-β''-Al_2O_3 powders meshed with mesh size lower than 0.5 mm. The 3D models consisted in more than 285000 and 355000 elements and in more than 720000 and 900000 degrees of freedom for 2450 MHz and 5800 MHz frequencies respectively. The simplified numerical simulation involved the use of the predefined RF (electromagnetic) application mode of COMSOL Multiphysics® v.3.3a [49]. The Pardiso direct solver [50] was used to numerically simulate the microwaves power density distribution into all the components of the load during the very early stages of sintering. The relevant materials properties considered in the model are reported in **Table 2**. For the numerical simulation reported herein, only the dielectric properties at room temperature and at 200°C were considered, and no temperature- nor frequency-dependence of permittivity of the extremely low loss refractory lining was assumed. Further assumptions include that the microwave source is operating at the nominal frequency (which is typical of solid state generators and not of magnetrons, like the ones used in this

study) and no load shape change occurs (which in fact happens as only the very beginning of the heating has been modelled). The boundary conditions set in the RF application mode for the external walls of both the microwave applicators are those of a perfect electrical conductor (P.E.C.), except for the microwave input ports where sinusoidal 2450MHz and 5800 MHz excitations in the TE_{10} mode were respectively set.

Table 2. Model components and relevant properties.

Component	Material	Properties @ 2450 MHz		Properties @ 5800 MHz	
		ε*@R.T =ε';ε"$_{eff}$	ε*@200°C =ε';ε"$_{eff}$	ε*@R.T =ε';ε"$_{eff}$	ε*@200°C=ε';ε"$_{eff}$
MWs coabsorber	SiC	9.3;1.2[51]	14.5;7.7 [51]	12;2.3[52]	15.2;6.1[52]
Compacted powders	Na-β''-Al_2O_3	2.5;0.04	3.37;0.26	1.7;0.45	2.81;0.95

Data for SiC at 200°C, 5.8 GHz, have been extrapolated from ref. 52 assuming a temperature dependence similar to the trend observed at 2.45 GHz

2.3 Characterization

The obtained powders were characterized in terms of particle size distribution by means of light scattering (Fraunhofer optical model, Malvern, Mastersizer 2000). Crystal structure and phase purity information of calcined powders and sintered samples were obtained by XRD analyses by using a Philips X'PERT PW 3710 diffractometer with Bragg–Brentano geometry, employing a Cu anode X-ray tube operating at 40 kV and 30 mA. Sintered samples were grinded and sieved through a 75 μm mesh in order to obtain fine powders for XRD analyses. Powder X-ray diffraction patterns were recorded at room temperature using a step scan procedure (0.03°/2θ step, 4 s time per step) in the 2θ range of 5–80°. Samples were spun during measurements. Rietveld refinements on X-ray powder

diffraction patterns were performed using MAUD software by using the full-profile fitting method [53].

The real density of the powders was determined by a Micromeritics AccuPyc II 1340 He pycnometer while the densification degree was evaluated by means of geometrical measurements of sintered samples.

The microstructures of the fresh fractured sintered specimens were observed by field emission scanning electron microscopy (FE-SEM) with a SIGMA Zeiss instrument (Carl Zeiss SMT Ltd, UK), equipped with a field emission gun, operating in high vacuum condition at an accelerating voltage variable from 0.2 to 30 kV.

3. Results and discussion

3.1 Powders characterization

The optimized synthetic procedure reported in [45] allowed obtaining the pure β''-Al_2O_3 crystalline phase, type $Na_{1.67}Li_{0.33}Al_{10.67}O_{17}$, having hexagonal cell geometry and *R-3m* space group (NaBA powders, **Table 3**). The further milling procedure (NaBA-DM powders) did not affect the crystal phase distribution, as shown in Figure S1 (Supporting Information) and quantitatively confirmed by the Rietveld refinement data reported in **Table 3**. On the contrary, the further ball milling treatment affected the particles size distribution, as expected. A bimodal distribution was exhibited by the frequency curves of both kinds of powders, from which the D10, D50, D90 and D100 values of **Table 3** were calculated.

Table 3. Rietvield refinement data and characteristic diameters of both as synthesized (NaBA) and further ball milled (NaBADM) Na-β''-Al_2O_3 powders.

Powders acronym	β″ phase			Grain size			
	(%vol)	a (Å)	c (Å)	D10 (μm)	D50 (μm)	D90 (μm)	D100 (μm)
NaBA	100	5.6131 [45]	33.8700 [45]	1.515	17.967	52.008	104.961
NaBA-DM	100	5.6050	33.8009	1.124	7.457	28.134	66.226

Theoretical density of the as-synthesized (NaBA) powders resulted 3.177 ± 0.004 g/ml, while the value for the further milled powders (NaBADM) resulted 3.019 ± 0.002 g/ml. These values are very close to the ones reported in the literature [45,54].

Real and imaginary parts of the complex dielectric permittivity of the as-synthesized Na-β''-Al_2O_3 powders (at 2470 MHz over the temperature range 20-1200°C) are reported in **Figure 3.** The results obtained at 5800 MHz frequency using the open-ended coaxial cable technique are reported in **Figure 4**. The room temperature loss tangent values resulted 0.018 at 2450 MHz and 0.268 at 5800 MHz. Therefore, Na-β''-Al_2O_3 powder can be considered low and medium microwave absorbing material, at the two investigated frequencies of 2450 MHz and 5800 MHz respectively, according to several classifications [55,56]. However, at 2450 MHz the microwave absorbing behavior of Na-β''-Al_2O_3, turns to one typical of medium microwave absorbing materials, as the temperature increases.

3.2 2450 MHz microwave assisted sintering experiments

Sintering experiments at 2450 MHz were performed in the microwave single mode applicator reported on the left side of **Figure 1a**. First sintering attempts were performed by exploiting the direct interaction of the electromagnetic field with the sample, without the help of any auxiliary co-absorbers. In these cases, the sample was simply positioned in the middle of the single mode cavity surrounded by a refractory and MW-transparent basement.

This configuration, however, resulted in un-controllable processes due to the fact that the temperature was the highest at the centre of the specimen, leading to thermal runaway (**Figure 5a**), that

significantly affected the microstructure of the sample, resulting in an evident density gradient (**Figure 5b**), with some regions even characterized by a microstructure typical of the occurrence of melting phenomena (**Figure 5c**).

Due to the difficulty to perform well-controlled sintering experiments by direct interaction of microwaves with the powder compacts, the use of silicon carbide co-absorber components was deemed necessary, thus hybrid sintering experiments were performed. The summary of the results obtained with this configuration at 2450 MHz is reported in the following **Table 4**.

Table 4. Densification and Rietveld refinement results for 2450 MHz microwave assisted sintered specimens.

Sample	T (°C)	Holding time (min)	Geometrical density (g/ml)	Relative density (%)	β″ phase		
					(%vol)	a (Å)	c (Å)
NaBA_01	1200	5	1.79	56	99	5.6151	33.9494
NaBA_02	1200	10	1.70	54	98.5	5.6168	33.9652
NaBA_03	1200	20	1.69	53	97.5	5.6165	33.9636
NaBA_04	1250	60	1.83	58	98.5	5.6159	33.9600
NaBA_05	1270	30	2.14	67	97	5.6137	33.8762
NaBA_06	1300	5	1.92	60	97.5	5.6169	33.9539
NaBA_07	1300	10	2.34	74	98	5.6169	33.9010
NaBA_08	1300	40	2.66	84	98.5	5.6063	33.6859
NaBADM_01	1300	10	2.54	84	99	5.6166	33.9412
NaBADM_02	1300	40	2.59	86	95.5	5.6168	33.8262

Satisfactory densification values, *i.e.* close to 90% of the theoretical were reached only at 1300°C both for NaBA and NaBA-DM powders. Indeed, from the results summarized in **Table 4**, temperatures of 1200 and 1250 °C are not sufficient to promote the starting of densification phenomena in the studied powders (at least up to 60 min holding time). Indeed, sintering treatments

at 1200°C for 5, 10 and 20 minutes respectively led to geometrical density values similar to those of the green not sintered specimens. The obtained typical microstructure is reported in **Figure 6a**, for the cross section of sample NaBA_01 which was chosen as representative example of this set of specimens. The increase of sintering temperature up to 1250°C did not lead to significant densification increase even by prolonging the heat treatment for 60 min as clearly evidenced by the cross-section microstructure of NaBA_04 specimen, reported in **Figure 6b**.

Only at 1270 °C and with an isothermal treatment of 30 min, the starting of densification is observed in some regions of the specimen NaBA_05 (leading to a relative density of 67% of theoretical).

Particularly, **Figure 7a** refers to one of these latter regions where sintering started, leading of course to a morphology completely different from those of completely un-sintered samples (as those reported in **Figure 6**). However, the sample treated at 1270 °C for 30 min (i.e. NaBA_05) results particularly not-homogeneous and regions completely un-sintered can be also detected, as the one reported in **Figure 7b**. As mentioned above, the most effective temperature in promoting sintering of the tested specimens was 1300°C. Moreover, a regular increase of the densification degree with increasing dwell time was detected, as can be observed in **Figure 8**, where the SEM micrographs of NaBA_06, NaBA_07 and NaBA_08 samples are reported. Indeed, by prolonging the dwell time at 1300°C from 5 (NaBA_06) to 10 (NaBA_07) and finally to 40 min (NaBA_08), the relative density increased from 60, to 74 and 84% respectively. Particularly, only when the thermal treatment at 1300 °C is prolonged from 3 (**Fig. 8a**) to 10 min (**Fig. 8b**) a beginning of the densification process is observed (**Fig. 8b1**), even if it is not complete, with several regions of the sample remaining un-sintered (**Fig. 8b2**). By prolonging the microwave assisted heating experiment for 40 min. a more homogeneous microstructure characterized by a good level of densification can be obtained (**Fig. 8c**).

On the contrary, an acceptable densification degree of NaBADM powders (i.e. subjected to a further ball milling treatment after calcination) was reached in only 10 min of holding time at 1300°C with a relative density value of 84 %, which is the same obtained at 1300°C for 40 min with NaBA powders. The corresponding microstructure is reported in **Figure 9a**. By prolonging the holding time

at 1300°C for up to 40 min, only a slight increase in the relative density was obtained, i.e. 86% for the NaBADM_02 sample, whose typical microstructure is reported in **Figure 9b**.

The Rietveld refinement data for all the samples sintered at 2450 MHz frequency are also reported in **Table 4**. In the collected spectra no signals arising from β' phase ($Al_{22}Na_2O_{34}$, with hexagonal cell, P63/mmc space group) could be detected except for the NaBADM02 sample that was treated for long time combined with high temperature. In this case, typical peaks of β' phase can be detected, as visible in **Figure 10**, where the XRD patterns of selected sintered specimens are reported as representative examples. Hence, it could be concluded that the microwave-assisted sintering did not lead to significant variations in the phase distribution with respect to the starting loose powders, with a volume percentage of Na-β''-Al_2O_3 phase exceeding in all cases 95%**.**

The claimed high degree of controllability for the hybrid sintering experiments performed in the present work by means of a microwave single mode applicator is confirmed and is easily inferable by the temperature and power profiles reported in **Figure 11** and referred to the sample NaBADM_02. Particularly, from those experimental data a total energy consumption of *ca*. 2.15 MJ was calculated, increasing to *ca*. 3.07 MJ by considering an average magnetron efficiency of 70%. Due to the mass of the sample heated (i.e. 1g), the latter value corresponds also to the specific energy consumption value (i.e. 3.07 MJ/g of NaBADM_02 specimen treated).

3.3 Preliminary 5800 MHz microwave assisted sintering experiments

Preliminary sintering experiments at 5800 MHz were performed in the microwave single mode applicator reported on the right side of **Figure 1a**. Again, load arrangement was designed in order to realize a hybrid microwave sintering configuration (see **Figure 1b** and **Table 1** for details), as the case of 2450 MHz experiments.

Due to the higher strength of the electric field, typical of higher frequencies, the maintenance of the selected sintering temperature (i.e. 1300°C) proved very difficult, due to the occurrence of arcing phenomena that significantly affected both the possibility to perform heating treatments for prolonged

times as well as the integrity of the sintered specimen. The results of the sole preliminary experiment performed at this frequency that allowed a well sintered and intact specimen to be obtained are reported in **Table 5**, while the cross-section microstructure of the NaBADM_03 specimen is reported in **Figure 12**. Similar conclusions to those made for samples sintered at 2450 MHz can be drawn: particularly, only some traces of β' phase could be detected for NaBADM_03 sample as observable from **Figure S2** (Supporting information).

Table 5. Densification and Rietvield refinement results for the 5800 MHz microwave assisted sintered specimen.

Sample	T (°C)	Holding time (min)	Geometrical density (g/ml)	Relative density (%)	β″ phase		
					(%vol)	a (Å)	c (Å)
NaBADM_03	1300	3	2.79	92	97.5	5.6064	33.7616

At 5800 MHz, it was possible to reach 1300°C and maintain it for approximately 3 min., by exploiting a forward microwave power of 250 W. However, as is visible from **Figure 13**, the temperature during this holding period, exhibited significant oscillation, exceeding 1400°C.

Irrespectively of the sintering temperature, the total energy consumption for this experiment (calculated from the power vs. time plot of **Figure 13**) was 0.19 MJ, increasing to 0.27 MJ considering the 70% efficiency of the microwave generator. This value, which corresponds also to the specific energy consumption is significantly lower compared to the best scenario of 2450 MHz, leading to the highest relative density value (i.e. 92%). Despite allowing more realistic energy efficiency comparisons between different microwave assisted sintering strategies with respect to comparisons simply based on temperature measurements, these preliminary specific energy consumption evaluations will, in all likelihood, enable more trustworthy comparisons including also conventional [45] as well as other innovative approaches, such as spark plasma sintering [57].

4. Numerical simulation results

The dielectric properties measured at ambient and 200°C were used to compute the electromagnetic field distribution inside the loaded cavities during the early stages of microwave assisted sintering experiments at both frequencies. This allowed the estimation of the microwave power density distributions into all the different components of the load and particularly the compacted Na-β''-Al_2O_3 powders, and subsequently an investigation of the homogeneity of the microwave treatment. Optimal impedance matching between the load and the microwave source at the two different frequencies investigated (as well as at both temperatures considered), was obtained by including in the model geometry a shorting plunger and a three stubs tuner (reflecting what has been performed manually during the sintering experiments).

The calculated S_{11} (i.e. the reflection coefficient on the sole microwave output port) parameters as a function of the input frequency, for the two different loaded cavities at ambient and 200°C are reported in **Figures S3** and **S4** respectively.

Under these optimized conditions 3D simulations using the RF module were conducted in order to obtain the power density distributions in the specimen (**Figure 14**), limited to the very first stages of sintering (i.e. up to 200°C).

In order to more accurately investigate the degree of homogeneity of the microwave heating treatments, the power density values (at both frequencies and both temperatures modelled) were analysed in a mid-horizontal cross section of the compacted Na-β''-Al_2O_3 powders to calculate the coefficient of variation (C.O.V.), which provides a statistical measure for non-uniformity [57]. From the results summarized in **Table 6**, microwave assisted hybrid heating experiments resulted to a good level of uniformity in power density distribution values when performing the experiments at 2450 MHz. Indeed, C.O.V. of 14.3% and 18.1% were calculated at room temperature and 200°C respectively. The uniformity in microwave power density distribution significantly decreases at 5800 MHz, as confirmed by the C.O.V., with a value of 82.2% at 25°C, decreasing to 48.6% at 200°C.

The results of the simplified numerical simulation can explain some of the experimental results obtained. Indeed, the not perfectly homogeneous power density distribution into the specimen to be

sintered (at least up to 200°C) can explain the small non-uniformities in the microstructures observed for most of the sintered specimens (even if hybrid microwave sintering is applied), thus affecting the final relative density values. Similarly, the higher coefficient of variation calculated in the case of 5800 MHz, can justify the significantly lower degree of controllability of the preliminary experiments performed, and therefore the extensive occurrence of arcing and thermal runaway phenomena that significantly limited the number of experiments feasible at this frequency for the obtainment of entire and intact samples with good reproducibility of results.

Table 6. Microwave power density values (at both frequencies and both temperatures modelled) analysed in a mid-horizontal cross section of the compacted Na-β''-Al_2O_3 powders, and calculated mean, standard deviation and coefficient of variation.

2450 MHz	
R.T.	**200°C**
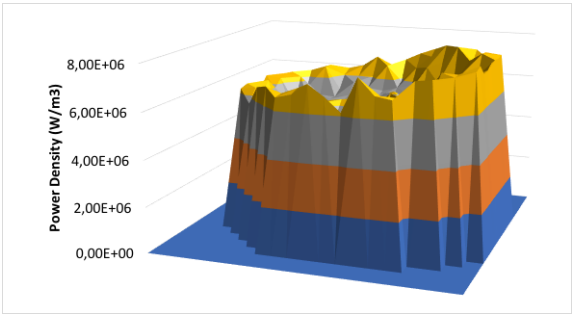	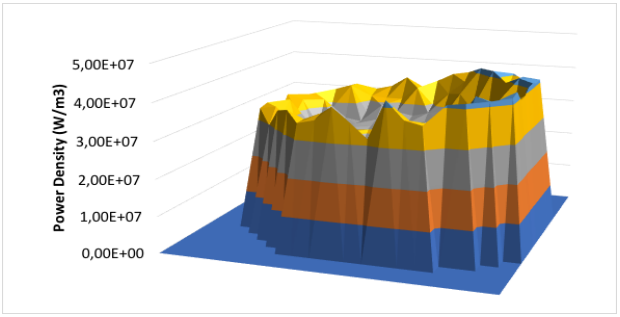
Mean = 6.11E+06 W/m^3; Std. Dev. = 8.76E+05 W/m^3; C.O.V. = 0.143;	Mean = 3.11E+07 W/m^3; Std. Dev. = 5.62E+06 W/m^3; C.O.V. = 0.181;
5800 MHz	
R.T.	**200°C**
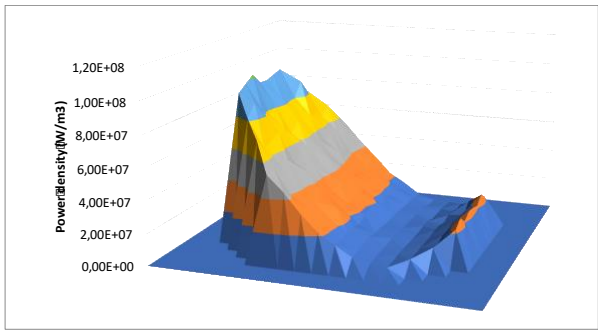	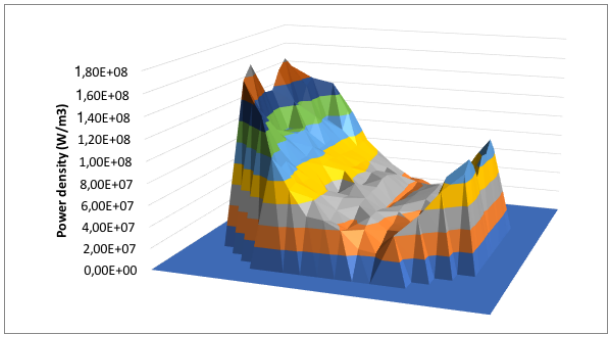
Mean = 3.25E+07 W/m^3; Std. Dev. = 2.68E+07 W/m^3; C.O.V. = 0.822;	Mean = 6.69E+07 W/m^3; Std. Dev. = 3.25E+07 W/m^3; C.O.V. = 0.486;

Conclusions

Microwave assisted sintering experiments of pure Na-β”-Al_2O_3 powders were performed, for the first time, in an extremely controlled manner at 2450 MHz frequency, due to the use of single mode applicator. By using this type of applicator, in addition to monitor accurately the surface temperature, it was also possible to measure continuously the forward power, that was used to calculate the specific energy consumptions, enabling future comparisons of the microwave assisted sintering approaches, proposed herein, with both traditional and new innovative sintering techniques, in terms of energy efficiency.

In addition to the widely used ISM (i.e. allowed for Industrial Scientific and Medical applications) frequency of 2450 MHz the less common one of 5800 MHz was also evaluated in preliminary sintering experiments. The use of both frequencies resulted to sintered ceramics almost exclusively characterized by the presence of the desired β” phase, exceeding in all cases the 95% of volume percentage. The latter result is particularly noteworthy, since conventional sintering approaches, which are generally carried out at temperatures of ca. 1600°C for prolonged periods of time, or with the help of sintering additives, typically promote the formation of a mixture of β’ and β” phases, and/or unwanted secondary phases.

A surface temperature of 1300°C was found to be necessary in order to reach satisfactory densification results (close to 90% of theoretical one). However, an isothermal treatment at 1300°C for 40 minutes was necessary to reach the best densification result at 2450 MHz. The use of Na-β”-Al_2O_3 powders subjected to a further milling procedure, allowed for a significant reduction (down to 10 min.) of the necessary residence time at the selected temperature to reach similar densification results, with only slight improvements obtained by further prolonging the isothermal treatment to 40 min.

When the 5800 MHz frequency was tested, it was possible to prolong the holding time at 1300 °C limitedly to 3 min without thermal runaway phenomena, leading to a relative density of 92%. Indeed, the use of this higher frequency resulted in the recurrent occurrence of arcing as well as thermal

runaway phenomena that affected the controllability of the heating treatment (even if performed under hybrid conditions) as well as the integrity of the treated specimens.

The experimental results obtained, have been subsequently analysed in more detail with the help of a simplified numerical simulation. The dielectric properties as a function of temperature of Na-β”-Al_2O_3 were used in order to design model geometries reproducing the experimentally employed ones. Simulations calculated the microwave power density distributions into the specimen to be sintered and provided insights on how the inhomogeneous microstructure detected in most of the sintered specimens could be a direct consequence of the non-uniform power density distribution inside the compacted powder mixtures. Particularly, the degree of non-uniformity, in the case of 5800 MHz microwave power density distribution was quantified in terms of the coefficient of variation as 82.2% and 48.6% for the room temperature and 200°C scenarios respectively, thus explaining the difficulties encountered in the performing of controllable experiments at this higher frequency.

In addition to providing accurate insights regarding the results experimentally obtained, the simplified model, developed herein, will contribute to the optimization of future microwave assisted sintering experiments, by evaluating the effect that load disposition, arrangement and amount have on the evaluation of non-uniformity in power density distributions within the samples.

References

[1] P. Pujar, B. Gupta, P. Sengupta, D. Gupta, S. Mandal, Sodium ion incorporated alumina - A versatile anisotropic ceramic, J. Eur. Cer. Soc., 39, 2019, 4473-4486.

[2] M. Beaudin, H. Zareipour, A. Schellenberglabe, W. Rosehart, Energy storage for mitigating the variability of renewable electricity sources: An updated review, Energy for Sustainable Development 14, 2010, 302-314.

[3] F. Díaz-González, A. Sumper, O. Gomis-Bellmunt, R. Villafáfila-Robles, Renewable and Sustainable Energy Reviews 16, 2012, 2154-2171.

[4] W. Hou, X. Guo, X. Shen, K. Amine, H. Yu, J. Lu, Solid electrolytes and interfaces in all-solid-state sodium batteries: Progress and perspective, Nano Energy 52, 2018, 279-291.

[5] K.B. Hueso, M. Armand, T. Rojo, High temperature sodium batteries: status, challenges and future trends, Energy. Environ. Sci. 6, 2013, 734-749.

[6] X. Lu, G. Xia, J.P. Lemmon, Z. Yang, Advanced materials for sodium-beta alumina batteries: Status, challenges and perspectives, J. Power Source 195, 2010, 2431-2442.

[7] J.T. Kummer, N. Weber, U.S. Patent 3,413,150 (1968).

[8] Z. Wen, J. Cao, Z. Gu, X. Xu, F. Zhang, Z. Lin, Research on sodium sulfur battery for energy storage, Solid State Ionics 179, 2008, 1697-1701.

[9] J.T. Kummer, in: H. Reiss, J.O. McCaldin (Eds.), Beta-Alumina Electrolytes, Pergamon Press, New York, 1972, pp. 141-175.

[10] B.L. Ellis, L.F. Nazar, Sodium and sodium-ion energy storage batteries, Current Opinion Solid State Mater. Sci. 16, 2012, 168-177.

[11] E. Yi, E. Temeche, R.M. Laine, Superionically conducting β’’-Al2O3 thin films processed using flame synthesized nanopowders, J. Mater. Chem. A 6, 2018, 12411-12419.

[12] B. Gupta, P. Pujar, S.S. Mal, D. Gupta, S. Mandal, Retention of high dielectric constant sodium beta alumina via solution combustion: Role of aluminum ions complexation with fuel, Ceram. Int. 44, 2018, 1500-1511.

[13] B.N. Pal, B.M. Dhar, K.C. See, H.E. Katz, Solution-deposited sodium beta-alumina gate dielectrics for low-voltage and transparent field-effect transistors, Nature Mater. 8, 2009, 898‑903.

[14] C. Schwandt, R. Vasant Kumar, M. P. Hills, Solid state electrochemical gas sensor for the quantitative determination of carbon dioxide, Sensors and Actuators B 265, 2018, 27–34.

[15] T. Oshima, M. Kajita, A. Okuno, Development of sodium-sulfur batteries, Int. J. Appl. Ceram. Technol. 1, 2004, 269-276.

[16] V. Jayaraman, T. Gnanasekaran, G. Periaswami, Low-temperature synthesis of beta-aluminas by a sol-gel technique, Mater. Lett. 30, 1997, 157-162.

[17] J. Lin, Z. Wen, X. Wang, S. Song, Y. Liu, Mechanochemical synthesis of Na-β/β’’-Al_2O_3, J. Solid State Electrochem. 14, 2010, 1821-1827.

[18] A. Mali, A. Petric, Synthesis of sodium β’’-alumina powder by sol-gel combustion, J. Eur. Ceram. Soc. 32, 2012, 1229-1234.

[19] T. Mathews, Solution combustion synthesis of magnesium compensated sodium-β-aluminas, Mater. Sci. Eng. B 78, 2000, 39-43.

[20] G. Chen, J. Lu, X. Zhou, L. Chen, X. Jiang, Solid-state synthesis of high performance Na-β″-Al_2O_3 solid electrolyte doped with MgO, Ceram. Int. 42, 2016, 16055-16062.

[21] C. Zhou, Y. Hong, P. Huang, Synthesis and characterization of NiO doped beta-Al_2O_3 solid electrolyte, J. Alloys Compds. 688, 2016, 746-751.

[22] D.H. Lee, S.T. Lee, J.S. Kim, S.K. Lim, Analysis of properties of partially stabilized zirconia-doped Na+-beta-alumina prepared by calcining-cum-sintering process, Mater. Res. Bull. 96, 2017, 143-148.

[23] K. Zhao, Y. Liu, S.M. Zeng, J.H. Yang, Y.W. Liu, Z.L. Zhan, L.J. Song, Preparation and characterization of a ZrO_2–TiO_2-co-doped Na-β″-Al_2O_3 ceramic thin film, Ceram. Int. 42, 2016, 8990-8996.

[24] X. Lu, G. Li, J.Y. Kim, K.D. Meinhardt, V.L. Sprenkle, Enhanced sintering of ß"-Al_2O_3/YSZ with the sintering aids of TiO_2 and MnO_2, J. Power Sources 295, 2015, 167-174.

[25] S. Barison, M. Fabrizio, S. Fasolin, F. Montagner, C. Mortalò, A microwave-assisted sol–gel Pechini method for the synthesis of $BaCe_{0.65}Zr_{0.20}Y_{0.15}O_{3-\delta}$ powders, Mater. Res. Bull. 45, 2010, 1171-1176.

[26] S. Boldrini, C. Mortalò, S. Fasolin, F. Agresti, L. Doubova, M. Fabrizio, S. Barison, Influence of microwave-assisted Pechini method on $La_{0.80}Sr_{0.20}Ga_{0.83}Mg_{0.17}O_{3-\delta}$ ionic conductivity, Fuel Cells 12, 2012, 54-60.

[27] D.K. Agrawal, Microwave processing of ceramics, Curr. Opinion Solid State Mater. Sci. 3, 1998, 480-485.

[28] C. Monaco, F. Prete, C. Leonelli, L. Esposito, A. Tucci, Microstructural study of microwave sintered zirconia for dental applications, Ceram. Int. 41, 2015, 1255-1261.

[29] R. Taurino, A. Karamanov, R. Rosa, E. Karamanova, L. Barbieri, S.A. Vladimirova, G. Avdeev, C. Leonelli, New ceramic materials from MSWI bottom ash obtained by an innovative microwave-assisted sintering process, J. Eur. Ceram. Soc. 37, 2017, 323-331.

[30] L. Gil-Flores, M.D. Salvador, F.L. Penaranda-Foix, A. Fernandez, M. Suarez, R. Rosa, P. Veronesi, C. Leonelli, A. Borrell, Microstructure and mechanical properties of 5.8 GHz microwave-sintered ZrO_2/Al_2O_3 ceramics, Ceram. Int. 45, 2019, 18059-18064.

[31] R. Roy, D. Agrawal, J. Cheng, S. Gedevanishvili, Full sintering of powdered-metal bodies in a microwave field, Nature 399, 1999, 668-670.

[32] K. Saitou, Microwave sintering of iron, cobalt, nickel, copper and stainless steel powders, Scripta Materialia 54, 2006, 875-879.

[33] C. Leonelli, P. Veronesi, L. Denti, A. Gatto, L. Iuliano, Microwave assisted sintering of green metal parts, J. Mater. Process. Technol. 205, 2008, 489-496.

[34] Y.D. Peng, J.H. Yi, S.D. Luo, L.Y. Li, G. Chen, J.M. Ran, Review of microwave energy application in metallic materials preparation, Rare Metal Mater. Eng. 38, 2009, 742-747.

[35] D. Demirskyi, D. Agrawal, A. Ragulya, Densification kinetics of powdered copper under single-mode and multimode microwave sintering, Mater. Lett. 64, 2010, 1433-1436.

[36] F. Xu, Y. Li, X. Hu, Y. Niu, J. Zhao, Z. Zhang, In situ investigation of metal's microwave sintering, Mater. Lett. 67, 2012, 162-164.

[37] K. Rodiger, K. Dreyer, T. Gerdes, M. Willert-Porada, Microwave sintering of hardmetals, Int. J. Refr. Metals Hard Mater. 16, 1998, 409-416.

[38] X. Zhou, L. Shen, L. Li, S. Zhou, T. Huang, C. Hu, W. Pan, X. Jing, J. Sun, L. Gao, Q. Huang, Microwave sintering carbon nanotube/$Ni_{0.5}Zn_{0.5}$Fe2O4 composites and their electromagnetic performance, J. Eur. Ceram. Soc. 33, 2013, 2119-2126.

[39] S. Jayalakshmi, S. Gupta, S. Sankaranarayanan, S. Sahu, M. Gupta, Structural and mechanical properties of $Ni_{60}Nb_{40}$ amorphous alloy particle reinforced Al-based composite produced by microwave-assisted rapid sintering, Mater. Sci. Eng. A 581, 2013, 119-127.

[40] M. Oghbaei, O. Mirzaee, Microwave versus conventional sintering: A review of fundamentals, advantages and applications, J. Alloys Compds. 494, 2010, 175-189.

[41] K.I. Rybakov, E.A. Olevsky, E.V. Krikun, Microwave sintering: Fundamentals and modeling, J. Am. Ceram. Soc. 96, 2013, 1003-1020.

[42] H.S. Kalsi, M. Dutta, S.K. Sharda, G.K. Padam, N.K. Arora, B.K. Das, Fabrication and characterization of microwave sintered β''-Al_2O_3 tubes, J. Mater. Sci. Lett. 19, 2000, 1119-1121.

[43] R. Subasri, T. Mathews, O.M. Sreedharan, V.S. Raghunathan, Microwave processing of sodium beta alumina, Solid State Ionics 158, 2003, 199-204.

[44] R. Subasri, Investigations on the factors assisting a one-step synthesis cum sintering of sodium beta alumina using microwaves, Mater. Sci. Eng. B 112, 2004, 73-78.

[45] S. Barison, S. Fasolin, C. Mortalò, S. Boldrini, M. Fabrizio, Effect of precursors on β-alumina electrolyte preparation, J. Eur. Ceram. Soc. 35, 2015, 2099-2107.

[46] Agilent application note, Basics of Measuring the Dielectric Properties of Materials (http://www.agilent.com/home).

[47] M. Al-Harahsheh, S. Kingman, A. Saeid, J. Robinson, G. Dimitrakis, H. Halnawafleh, Dielectric properties of Jordanian oil shales, Fuel Process. Technol. 90, 2009, 1259-1264.

[48] M. Bhattacharya, T. Basak, A review on the susceptor assisted microwave processing of materials, Energy 97, 2016, 306-338.

[49] R. Rosa, P. Veronesi, S. Han, V. Casalegno, M. Salvo, E. Colombini, C. Leonelli, M. Ferraris, Microwave assisted combustion synthesis in the system Ti-Si-C for the joining of SiC: Experimental and numerical simulation results, J. Eur. Ceram. Soc. 33, 2013, 1707-1719.

[50] O. Schenk, K. Gartner, Solving unsymmetric sparse systems of linear equations with PARDISO, J. Future Gener. Comp. Syst. 20, 2004, 475-487.

[51] J. Robinson, S. Kingman, D. Irvine, P. Licence, A. Smith, G. Dimitrakis, D. Obermayer, C.O. Kappe, Electromagnetic simulations of microwave heating experiments using reaction vessels made out of silicon carbide, Phys. Chem. Chem. Phys. 12, 2010, 10793-10800.

[52] I. Polaert, N. Benamara, J. Tao, T-H. Vuong, M. Ferrato, L. Estel, Dielectric properties measurement methods for solids of high permittivities under microwave frequencies and between 20 and 250°C, Chem. Eng. Process. 122, 2017, 339-345.

[53] L. Lutterotti, S. Matthies, H.-R. Wenk, A.J. Schultz, J. Richardson, Combined texture and structure analysis of deformed limestone from time-of-flight neutron diffraction spectra, J. Appl. Physics, 1997, 81, 594.

[54] E. Mercadelli, A.S. Aricò, A. Gondolini, S. Siracusano, M. Ferraro, V. Antonucci, A. Sanson, Influence of powders thermal activation process on the production of planar β-alumina ceramic membranes, J. Alloys Compds. 696, 2017, 1080-1089.

[55] A. R. Von Hippel, Dielectric Materials and Applications, (2nd Edition) Artech House, Boston, MA, USA, 1995.

[56] R. Rosa, C. Ponzoni, P. Veronesi, I. Natali Sora, V. Felice, C. Leonelli, Solution combustion synthesis of La1-xSrxFe1-yCuyO3 ± w (x=0, 0.2; y=0, 0.2) perovskite nanoparticles: Conventional vs. microwaves ignition, Ceram. Int. 41, 2015, 7803-7810.

[57] K. Li, Y. Yang, X. Zhang, S. Liang, Highly oriented β''-alumina ceramics with excellent ionic conductivity and mechanical performance obtained by spark plasma sintering technique, J. Mater. Sci. (2020). https://doi.org/10.1007/s10853-020-04423-x.

[58] S. Geedipalli, A.K. Datta, V. Rakesh, Heat transfer in a combination microwave-jet impingement oven, Food Bioprod. Proc. 86, 2008, 53-63.

FIGURE CAPTIONS

Figure 1. (a) 2450 and 5800 MHz single mode cavities used for the microwave assisted sintering experiments. (b) The different components constituting the load inserted in the microwave single mode applicator for the hybrid sintering experiments (the case of 5800 MHz frequency applicator is reported as representative example). (c) The sapphire fibre used for surface temperature measurements inserted from the top of the rectangular single mode cavity (the case of 5800 MHz frequency applicator is reported as representative example).

Figure 2. 2450 MHz (a) and 5800 MHz (b) model geometries in which the dimensions are expressed in metres. Both loads are composed by the compacted Na-β''-Al_2O_3 powders (in red) surrounded by the SiC elements (blue), in turn contained in the Al_2O_3-based refractory container (transparent).

Figure 3. Temperature dependent 2470 MHz real (ε') and imaginary (ε'') parts of the complex dielectric permittivity.

Figure 4. Temperature dependent 5800 MHz real (ε') and imaginary (ε'') parts of the complex dielectric permittivity.

Figure 5. (a) Photograph showing the specimen heated by direct interaction with the 2450 MHz microwave field. As the temperature gradually increase, the central region of the specimen immediately results the hottest one, undergoing thermal runaway phenomena, resulting in a microstructure with an evident porosity gradient (b), with the inner region even melted (c).

Figure 6. SEM images of the cross sections of NaBA_01 (a) and NaBA_04 (b) specimens.

Figure 7. SEM images of the cross section of NaBA_05 collected from a well sintered area (a) and from a low density one (b).

Figure 8. SEM images of the cross sections of NaBA_06 (a), NaBA_07 (b1,2) and NaBA_08 (c).

Figure 9. SEM images of the cross sections of NaBADM_01 (a) and NaBADM_02 (b).

Figure 10. XRD patterns of selected specimens after 2450 MHz microwave assisted sintering experiments. *Refers to β'-Al_2O_3 phase (with hexagonal cell, P63/mmc space group) that was detected only in NaBADM_02 specimen.

Figure 11. Temperature and microwave power profiles experimentally collected during 2450 MHz microwave assisted sintering of NaBADM_02 sample.

Figure 12. SEM image of the cross section of sample NaBADM_03.

Figure 13. Temperature and microwave forward power profile experimentally collected during 5800 MHz microwave assisted sintering of NaBADM_03 sample.

Figure 14. Microwave power density distributions in the compacted Na-β''-Al_2O_3 powders at: (a) 2450 MHz / 25°C, (b) 2450 MHz / 200°C, (c) 5800 MHz / 25°C and (d) 5800 MHz / 200°C.